Supplemental Material

Maresin 1 Activates LGR6 Receptor Promoting Phagocyte Immunoresolvent Functions

Nan Chiang, Stephania Libreros, Paul C. Norris, Xavier de la Rosa, Charles N. Serhan

Center for Experimental Therapeutics and Reperfusion Injury, Department of Anesthesiology, Perioperative and Pain Medicine, Brigham and Women's Hospital and Harvard Medical School, Boston, Massachusetts 02115, USA.

Supplemental Table 1. Screening of orphan GPCRs with MaR1

GPCR ID	Vehicle Mean RLU	SD	Vehicle Mean RLU + 2 SD	MaR1 Mean RLU	% Activity	MaR1 mean RLU > Vehicle mean RLU+2 SD?
ADMR	930920	33283	997486.5381	863760	-7%	
BAI1	172580	18362	209304.1828	176160	2%	
BAI2	26390	1354	29097.71737	26240	-1%	
BAI3	18040	758	19555.07976	18460	2%	
CCRL2	15090	402	15893.6583	13840	-8%	
CMKLR2	30080	1744	33568.954	28240	-6%	
DARC	119110	4817	128743.8016	126260	6%	
EBI2	101200	6004	113207.8197	105640	4%	
GHSR1B	3940	203	4345.298244	3700	-6%	
GPR101	41740	1593	44926.97349	41580	0%	
GPR103	21413	1484	24381.25067	23920	12%	NO
GPR107	366800	11007	388814.4922	360020	-2%	
GPR12	77980	1563	81105.4653	76260	-2%	
GPR123	1485190	46446	1578081.986	1342640	-10%	
GPR132	860940	17473	895885.901	826560	-4%	
GPR135	18720	1656	22032.6827	17540	-6%	
GPR137	40973	2285	45544.0809	39140	-4%	
GPR139	438280	16736	471751.0542	413120	-6%	
GPR141	30180	2080	34339.2307	29020	-4%	
GPR142	105250	12089	129427.069	101020	-4%	
GPR143	89390	5260	99910.40557	89380	0%	
GPR146	16860	551	17961.75617	16240	-4%	
GPR148	6160	484	7128.848113	7520	22%	YES
GPR149	50140	934	52008.76073	49720	-1%	
GPR15	10110	1086	12282.67884	10300	2%	
GPR150	36470	2724	41918.3759	36340	0%	
GPR151	52730	3187	59104.07248	47340	-10%	
GPR152	141950	9317	160584.4913	138140	-3%	
GPR157	358200	14714	387627.8236	343680	-4%	
GPR161	8050	1129	10308.377	7220	-10%	
GPR162	14750	1297	17344.25005	15120	3%	
GPR17	1085570	20872	1127313.158	1045800	-4%	
GPR171	8100	601	9301.776463	9000	11%	NO
GPR173	87030	3746	94522.25378	81220	-7%	
GPR176	431010	17476	465962.1196	413620	-4%	
GPR18	3320	393	4106.553664	3220	-3%	
GPR182	749570	28457	806483.1034	714820	-5%	
GPR20	135610	4104	143817.2813	127200	-6%	
GPR23	1203410	43969	1291348.072	1204500	0%	
GPR25	4290	826	5942.956946	4500	5%	
GPR26	2160	287	2733.178274	2180	1%	
GPR27	163370	6480	176330.0617	159940	-2%	
GPR3	1808630	44214	1897058.155	1811960	0%	
GPR30	7130	688	8506.953158	6640	-7%	
GPR31	6130	388	6906.659514	5960	-3%	
GPR32	139240	5586	150411.392	141060	1%	
GPR37	993010	16495	1025999.138	973600	-2%	
GPR37L1	56170	2469	61107.74577	55060	-2%	
GPR39	469030	31072	531174.4125	456860	-3%	
GPR4	8760	1326	11411.69128	8200	-6%	
GPR45	925030	20094	965217.3147	926960	0%	
GPR50	792240	26238	844715.8941	829460	5%	
GPR52	8960	571	10101.46105	10060	12%	NO
GPR6	57570	1683	60936.58086	61040	6%	
GPR61	240140	15202	270544.8768	225800	-6%	
GPR65	73000	2702	78403.80113	68380	-6%	
GPR75	95540	6715	108969.4403	95760	0%	
GPR78	59770	2998	65765.33152	62160	4%	
GPR79	65520	1042	67603.07465	64880	-1%	
GPR81	485040	11086	507212.6558	486100	0%	
GPR83	91630	4012	99654.86137	89920	-2%	
GPR84	50450	1619	53688.68286	47200	-6%	
GPR85	10650	571	11791.46105	9740	-9%	
GPR88	27850	4137	36123.55627	25580	-8%	
GPR91	15520	1710	18940.40933	17840	15%	NO
GPR97	1006310	27047	1060403.977	989660	-2%	
LGR4	13700	2273	18246.41251	13560	-1%	
LGR5	5720	510	6740.326745	5040	-12%	
LGR6	16600	1130	18859.9115	19520	18%	YES
MRGPRD	11810	1431	14672.44651	11220	-5%	
MRGPRE	399420	13490	426400.4868	399320	0%	
MRGPRF	645150	22893	690936.7696	616940	-4%	
MRGPRX1	2179150	41244	2261637.058	2162000	-1%	
MRGPRX4	140390	7526	155442.2468	135940	-3%	
OPN5	13950	1064	16078.03509	13300	-5%	
OXGR1	187130	5028	197185.075	185060	-1%	
P2RY8	875740	12164	900068.1127	844400	-4%	
TAAR5	2430	229	2888.984386	2030	-16%	

Using β-arrestin PathHunter GPCR system, a panel of orphan GPCRs (77 GPCRs) was screened in the presence of 10 nM of MaR1 or vehicle control (0.1 % ethanol). The % activity = 100% x (mean RLU of test sample – mean RLU of vehicle control) / (mean RLU of vehicle control). RLU, relative luminescence units. Candidates were selected based on the criteria that the mean RLU in the presence of MaR1 is larger than the mean RLU +2 SD with vehicle alone

Supplemental Table 2. Screening of known GPCRs with MaR1

GPCR ID	% Activity	GPCR ID	% Activity	GPCR ID	% Activity	GPCR ID	% Activity
ADCYAP1R1	0%	CMKLR1	0%	GIPR	-7%	NPY1R	-1%
ADORA3	-1%	CMKOR1	-3%	GLP1R	0%	NPY2R	0%
ADRA1B	-3%	CNR1	-6%	GLP2R	-2%	NTSR1	0%
ADRA2A	0%	CNR2	0%	GPR1	0%	OPRD1	-1%
ADRA2B	0%	CRHR1	-1%	GPR109A	-2%	OPRK1	2%
ADRA2C	0%	CRHR2	0%	GPR119	-1%	OPRL1	-1%
ADRB1	0%	CRTH2	0%	GPR120	11%	OPRM1	0%
ADRB2	0%	CX3CR1	-10%	GPR35	0%	OXTR	0%
AGTR1	0%	CXCR1	-1%	GPR55	2%	P2RY11	-1%
AGTRL1	0%	CXCR2	0%	GPR92	-3%	P2RY12	-3%
AVPR1A	-1%	CXCR3	-2%	GRPR	1%	P2RY2	-2%
AVPR1B	1%	CXCR4	11%	HCRTR1	0%	P2RY4	-10%
AVPR2	-1%	CXCR5	-3%	HCRTR2	0%	P2RY6	-1%
BDKRB1	-1%	CXCR6	0%	HRH1	0%	PPYR1 (NPY4)	-2%
BDKRB2	-1%	DRD1	0%	HRH2	-2%	PRLHR	-4%
BRS3	5%	DRD2L	0%	HRH3	-1%	PROKR1	-1%
C5AR1	0%	DRD2S	-2%	HTR1A	-2%	PROKR2	-1%
C5LR2	-6%	DRD3	0%	HTR1B	-4%	PTAFR	1%
CALCR	1%	DRD4	-10%	HTR1E	3%	PTGER2	1%
CALCR + RAMP2	0%	DRD5	0%	HTR1F	2%	PTGER3	0%
CALCR + RAMP3	-7%	EDG1	0%	HTR2A	4%	PTGER4	0%
CALCRL + RAMP1	0%	EDG2	-6%	HTR2C	-3%	PTGIR	-1%
CALCRL + RAMP2	-1%	EDG3	-2%	HTR5A	-4%	PTHR1	0%
CALCRL + RAMP3	0%	EDG4	0%	KISS1R	3%	PTHR2	0%
CCKAR	0%	EDG5	-2%	LHCGR	8%	RXFP3	1%
CCKBR	2%	EDG6	-1%	LTB4R	-1%	SCTR	-1%
CCR10	-1%	EDG7	-1%	MC1R	-14%	SSTR2	0%
CCR2	-1%	EDG8	-8%	MC3R	-1%	SSTR3	2%
CCR3	4%	EDNRA	1%	MC4R	-3%	SSTR5	-1%
CCR4	-1%	EDNRB	0%	MC5R	-3%	TACR1	-4%
CCR5	-1%	F2R	-2%	MCHR1	-2%	TACR2	-2%
CCR6	0%	F2RL1	0%	MCHR2	-1%	TACR3	0%
CCR7	0%	F2RL3	0%	MLNR	0%	TBXA2R	-1%
CCR8	-1%	FPR1	0%	MRGPRX2	-3%	TRHR	-1%
CCR9	-1%	FPRL1	0%	MTNR1A	0%	TSHR	-2%
CHRM1	-3%	FSHR	2%	MTNR1B	0%	UTR2	-1%
CHRM2	1%	GALR1	0%	NMU1R	-2%	VIPR1	0%
CHRM3	-1%	GALR2	-3%	NPBWR1	-1%	VIPR2	0%
CHRM4	-3%	GCGR	-1%	NPBWR2	-1%		
CHRM5	6%	GHSR1A	-2%	NPFFR1	3%		

Using β-arrestin PathHunter GPCR system, a panel of known GPCRs (158 GPCRs) was screened in the presence of 10 nM of MaR1 or vehicle control (0.1 % ethanol). The % activity = 100% x (mean RLU of test sample – mean RLU of vehicle control) / (mean RLU of vehicle control). RLU, relative luminescence units.

Supplemental Table 3. AA, EPA and DHA bioactive metabolome

			LM levels (pg/ml)											
AA bioactive metabolome	**Q1**	**Q3**	**Mock transfection**			**LGR6 transfection**			**Mock transfection + E. coli**			**LGR6 transfection + E. coli**		
LXA_4	**351**	**115**	**18.5**	**±**	**12.6**	**15.6**	**±**	**10.7**	**24.9**	**±**	**17.3**	**19.0**	**±**	**13.3**
LXB_4	**351**	**221**	**1.6**	**±**	**1.1**	**1.3**	**±**	**0.9**	**2.3**	**±**	**1.9**	**0.9**	**±**	**0.6**
AT-LXA_4	**351**	**115**	**16.1**	**±**	**10.2**	**26.8**	**±**	**17.8**	**28.1**	**±**	**15.0**	**29.0**	**±**	**14.5**
AT-LXB_4	**351**	**221**	**102.4**	**±**	**46.7**	**115.4**	**±**	**53.8**	**85.1**	**±**	**41.4**	**101.5**	**±**	**46.7**
LTB_4	**335**	**195**	**11.8**	**±**	**6.8**	**9.9**	**±**	**5.6**	**56.4**	**±**	**47.4**	**60.5**	**±**	**55.9**
PGD_2	**351**	**233**	**54.8**	**±**	**22.0**	**55.7**	**±**	**19.6**	**70.7**	**±**	**27.9**	**73.7**	**±**	**27.5**
PGE_2	**351**	**189**	**51.3**	**±**	**16.3**	**51.2**	**±**	**14.4**	**58.4**	**±**	**22.2**	**59.2**	**±**	**16.7**
$PGF_{2\alpha}$	**353**	**193**	**129.6**	**±**	**43.0**	**104.8**	**±**	**29.9**	**155.9**	**±**	**48.0**	**111.7**	**±**	**35.7**
TXB_2	**369**	**169**	**2757.6**	**±**	**735.8**	**2935.5**	**±**	**805.6**	**3894.9**	**±**	**1151.8**	**3048.0**	**±**	**924.5**
DHA bioactive metabolome														
RvD1	**375**	**121**		**-**			**-**			**-**			**-**	
RvD2	**375**	**175**		**-**			**-**			**-**			**-**	
RvD3	**375**	**147**	**9.9**	**±**	**2.3**	**9.0**	**±**	**2.0**	**9.9**	**±**	**1.5**	**10.7**	**±**	**2.1**
RvD4	**359**	**255**		**-**			**-**			**-**			**-**	
RvD5	**359**	**199**	**2.7**	**±**	**0.7**	**2.3**	**±**	**0.4**	**3.9**	**±**	**0.8**	**2.7**	**±**	**0.6**
RvD6				**-**			**-**							
AT-RvD1	**375**	**121**	**7.0**	**±**	**5.6**	**6.9**	**±**	**4.7**	**6.2**	**±**	**5.8**	**5.8**	**±**	**4.2**
AT-RVD3	**375**	**147**	**0.6**	**±**	**0.4**	**0.4**	**±**	**0.2**	**0.7**	**±**	**0.4**	**0.9**	**±**	**0.6**
PD1	**359**	**153**	**0.4**	**±**	**0.1**	**0.2**	**±**	**0.1**	**0.6**	**±**	**0.3**	**0.3**	**±**	**0.1**
AT-PD1	**359**	**153**		**-**			**-**			**-**			**-**	
MaR1	**359**	**221**	**4.2**	**±**	**2.2**	**5.2**	**±**	**2.5**	**5.4**	**±**	**2.7**	**3.5**	**±**	**1.2**
EPA bioactive metabolome														
RvE1	**349**	**195**		**-**			**-**			**-**			**-**	
RvE2	**333**	**253**	**3.3**	**±**	**1.5**	**3.8**	**±**	**1.1**	**1.0**	**±**	**0.8**	**3.4**	**±**	**1.8**
RvE3	**333**	**201**	**19.3**	**±**	**4.0**	**21.1**	**±**	**4.7**	**23.4**	**±**	**4.5**	**24.3**	**±**	**5.6**

Human macrophages ($1x10^6$ cells) were transfected with mock or LGR6 (see Methods) for 3 days, followed by addition of E. coli ($50x10^6$ CFU) for 1h. Incubations were terminated by addition of 1V methanol with internal standards and extracted. LM levels were then determined using LM metabolopidomics (see Methods for details). Values are express as pg/ml ($0.5x10^6$ cells); mean ± SEM.

Supplemental Table 4. Sequences for shRNA knockdown*

Gene ID	shRNA.name	SplashRNA LGR6 Human	97mer.construct
59352	LGR6_59352_1160	1.503	TGCTGTTGACAGTGAGCGACCTGTGAGTACCTCTTT GAAATAGTGAAGCCACAGATGTATTTCAAAGAGGTA CTCACAGGGTGCCTACTGCCTCGGA
59352	LGR6_59352_454	1.495	TGCTGTTGACAGTGAGCGACAGGAGTTTCCAGATCT CAAATAGTGAAGCCACAGATGTATTTGAGATCTGGA AACTCCTGGTGCCTACTGCCTCGGA
59352	LGR6_59352_1743	1.357	TGCTGTTGACAGTGAGCGACGGTGCCTACATCAAAC TGTATAGTGAAGCCACAGATGTATACAGTTTGATGTA GGCACCGGTGCCTACTGCCTCGGA
59352	LGR6_59352_453	1.204	TGCTGTTGACAGTGAGCGCCCAGGAGTTTCCAGATC TCAATAGTGAAGCCACAGATGTATTGAGATCTGGAA ACTCCTGGATGCCTACTGCCTCGGA
59352	LGR6_59352_1159	1.093	TGCTGTTGACAGTGAGCGACCCTGTGAGTACCTCTT TGAATAGTGAAGCCACAGATGTATTCAAAGAGGTAC TCACAGGGCTGCCTACTGCCTCGGA
59352	LGR6_59352_825	0.933	TGCTGTTGACAGTGAGCGCTGGGGGCTTGATGCATC TGAATAGTGAAGCCACAGATGTATTCAGATGCATCAA GCCCCCAATGCCTACTGCCTCGGA
59352	LGR6_59352_1698	0.829	TGCTGTTGACAGTGAGCGACGTGGCCCTGGTGATG ATGAATAGTGAAGCCACAGATGTATTCATCATCACCA GGGCCACGGTGCCTACTGCCTCGGA
59352	LGR6_59352_6	0.793	TGCTGTTGACAGTGAGCGCCAGCATGAACAACCTCA CAGATAGTGAAGCCACAGATGTATCTGTGAGGTTGT TCATGCTGATGCCTACTGCCTCGGA
59352	LGR6_59352_1749	0.744	TGCTGTTGACAGTGAGCGACTACATCAAACTGTACT GTGATAGTGAAGCCACAGATGTATCACAGTACAGTT TGATGTAGGTGCCTACTGCCTCGGA
59352	LGR6_59352_1704	0.700	TGCTGTTGACAGTGAGCGACCTGGTGATGATGAACT CCTTTAGTGAAGCCACAGATGTAAAGGAGTTCATCAT CACCAGGGTGCCTACTGCCTCGGA
Control	Ren.713	Negative Control	TGCTGTTGACAGTGAGCGCAGGAATTATAATGCTTAT CTATAGTGAAGCCACAGATGTATAGATAAGCATTATA ATTCCTATGCCTACTGCCTCGGA

* obtained using software in ref 50.

Supplemental Table 5. Antibodies used in cyTOF

Target epitope	Clone	Isotopic label	Supplier
pAKT (S473)	D9E	Sm 152	Fluidigm
p-p38 (T180/Y182)	D3F9	Gd 156	Fluidigm
pStat3 (Y705)	4	Gd 158	Fluidigm
pStat1 (Y701)	58D6	Gd 160	BWH
pNF-κB p65 (S529)	K10-895.12.50	Er 166	Fluidigm
pERK (T202/Y204)	D13.14.4E	Er 167	Fluidigm
pS6 (S235/S236)	N7-548	Yb 172	Fluidigm
HLA-DR	L243	Yb 173	Fluidigm
pStat5 (Y694)	D47/E7 XP	Yb 174	BWH
pCREB (S133)	8763	Yb 176	Fluidigm

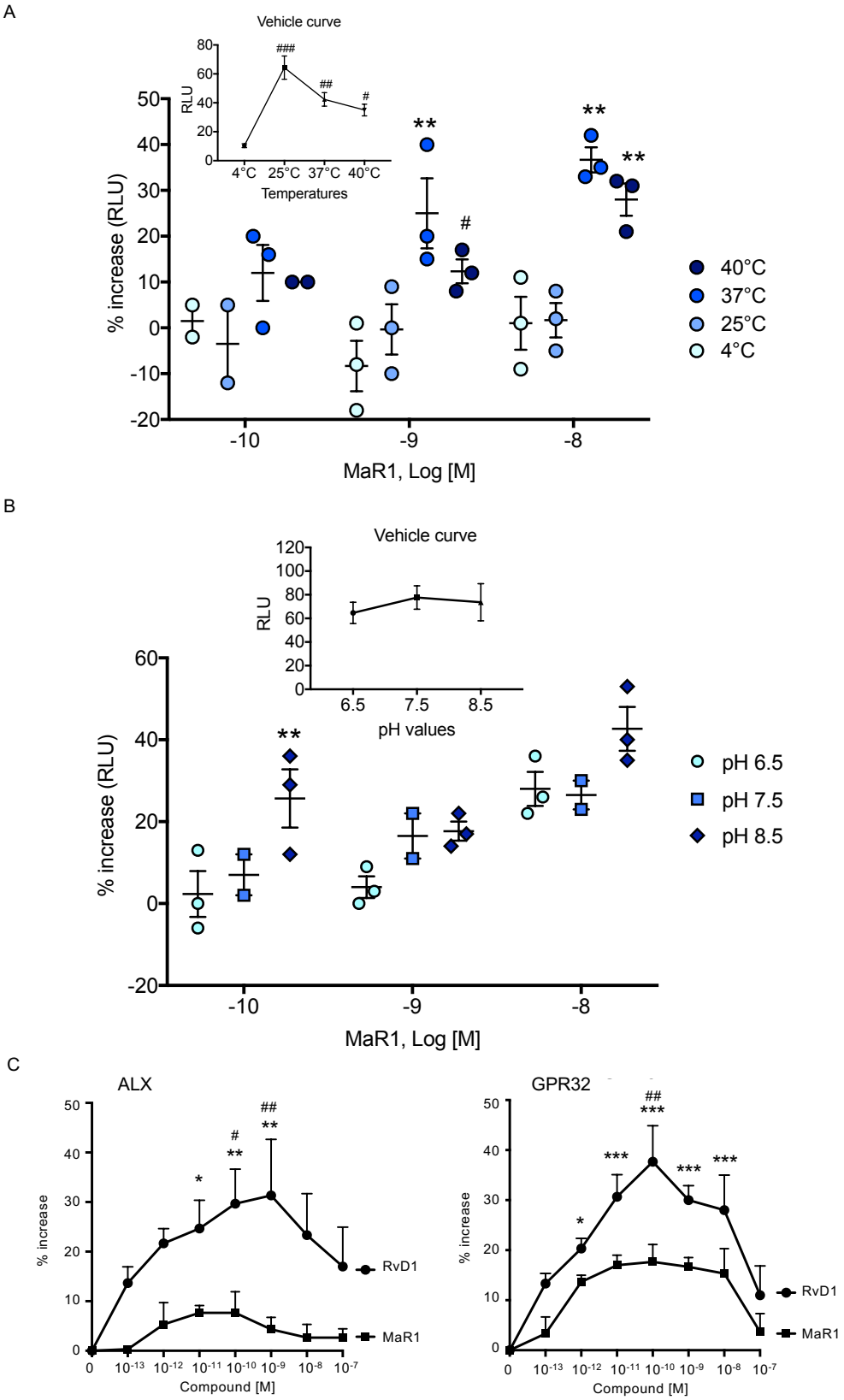

Supplemental Figure 1. MaR1 interactions with LGR6, ALX and GPR32

(A, B) MaR1-LGR6 interactions were monitored using CHO-β-arrestin-human LGR6 reporter cells under different temperatures (A, replotted from Figure 1F for direct comparison) and pH (B). Results are mean±SEM from 3 independent experiments and 3 replicates each experiment. (*insets*) vehicle curves under different temperatures and pH. (A) $^{\#}$P<0.05, $^{\#\#}$P<0.01, $^{\#\#\#}$P<0.001 vs 4°C, **P<0.01, vs 4°C and 25°C. (B) **P<0.01, pH 6.5 vs pH 8.5.

(C) MaR1 interactions with HEK-β-arrestin-ALX and CHO-β-arrestin-human GPR32 system, compared to RvD1. Results are mean±SEM from 3 independent experiments and 3-4 replicates for each experiment. *P<0.05, **P<0.01, ***P<0.001, vs vehicle control; $^{\#}$P<0.05, $^{\#\#}$P<0.01, vs MaR1. All panels were analyzed by two-way ANOVA with Tukey's multiple comparisons test.

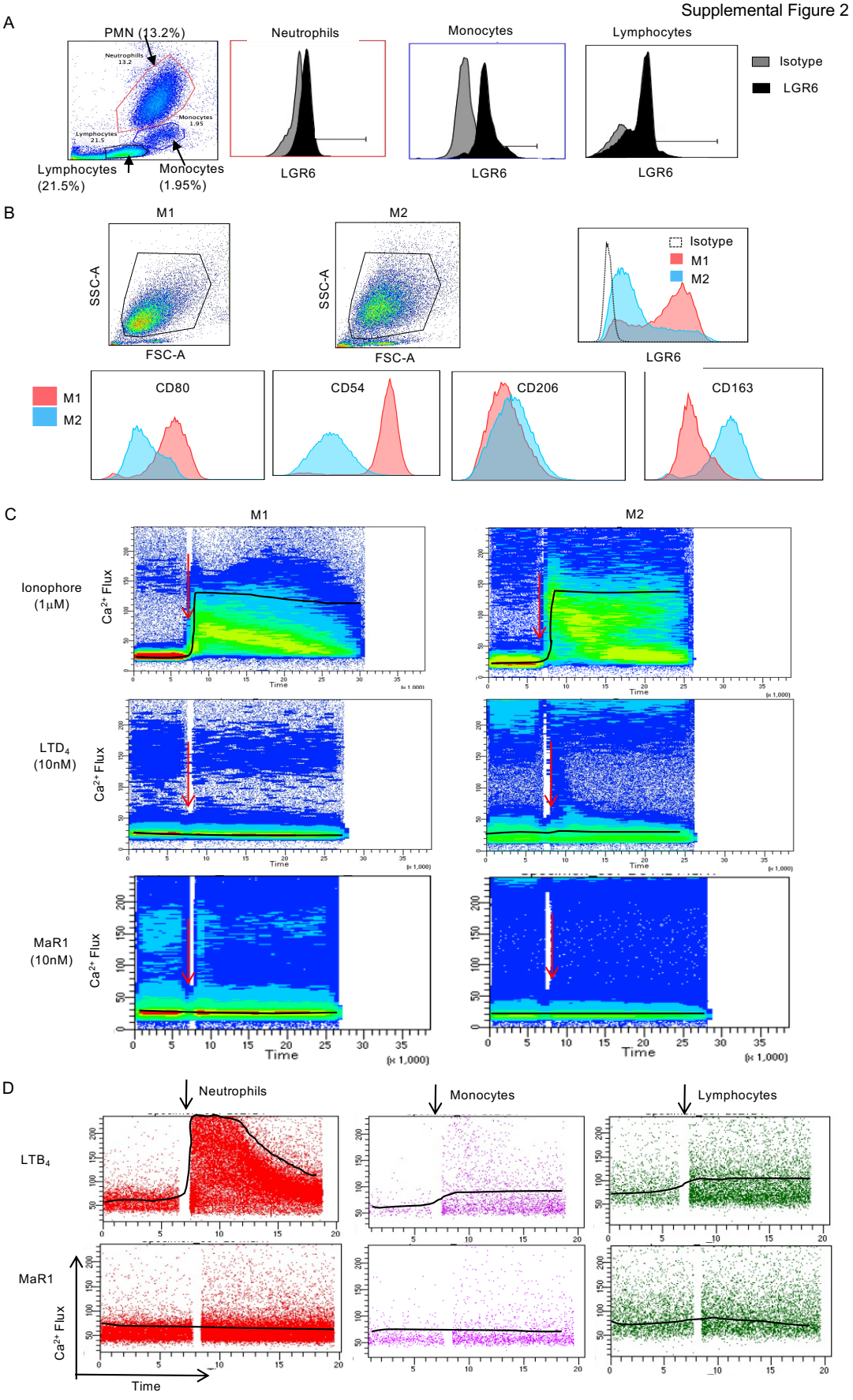

Supplemental Figure 2. Human leukocytes: LGR6 expression and intracellular calcium release (A) LGR6 expression in human peripheral blood leukocytes (PMN, monocytes and lymphocytes) was demonstrated using a rabbit anti-human LGR6 Ab by flow cytometry.

(B) LGR6 expression in M1 (CD80, CD54) and M2 (CD206, CD163) macrophages

(C, D) Calcium influx in (C) M1, M2 macrophages, and (D) peripheral blood leukocytes (PMN, monocytes and lymphocytes) was monitored using flow cytometry with a Indo-1 fluorescent indicator.

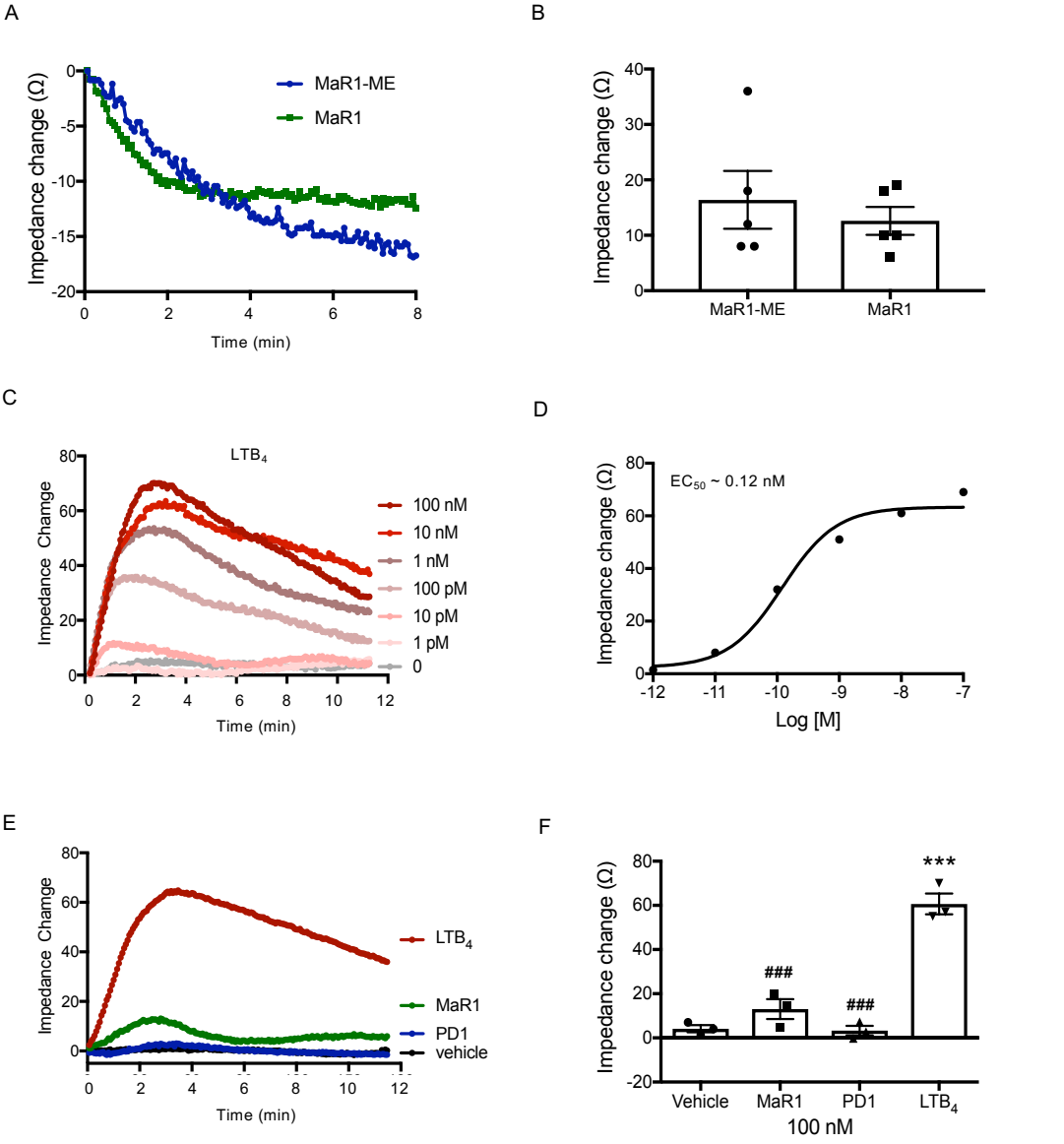

Supplemental Figure 3. Human recombinant LGR6 and BLT1 receptor specificity

(A, B) CHO-LGR6 cells were plated onto 8-well ECIS arrays (8W10E+), incubated with MaR1 (100 nM), MaR1-ME (100 nM) or vehicle alone (control), and impedance changes across CHO cell monolayers were continuously recorded every 4 seconds for 8 min using ECIS. Results are mean (A) or mean±SEM (B) of impedance changes; n=5. No statistical significance between MaR1 and MaR1-ME; two-tailed paired Student's t-test.

(C-F) CHO-BLT1 cells were plated onto 8-well ECIS arrays (8W10E+), incubated with (C,D) LTB_4 (0.001-100 nM), (E,F) MaR1, PD1, LTB_4 (100 nM) or vehicle alone (control), and impedance changes across CHO cell monolayers were continuously recorded every 4 seconds using ECIS. Results are mean (C,E) or mean±SEM (D,F) from n=3, ***P<0.001, vs vehicle; ###P<0.001, vs. LTB_4; one-way ANOVA with Tukey's multiple comparisons test.

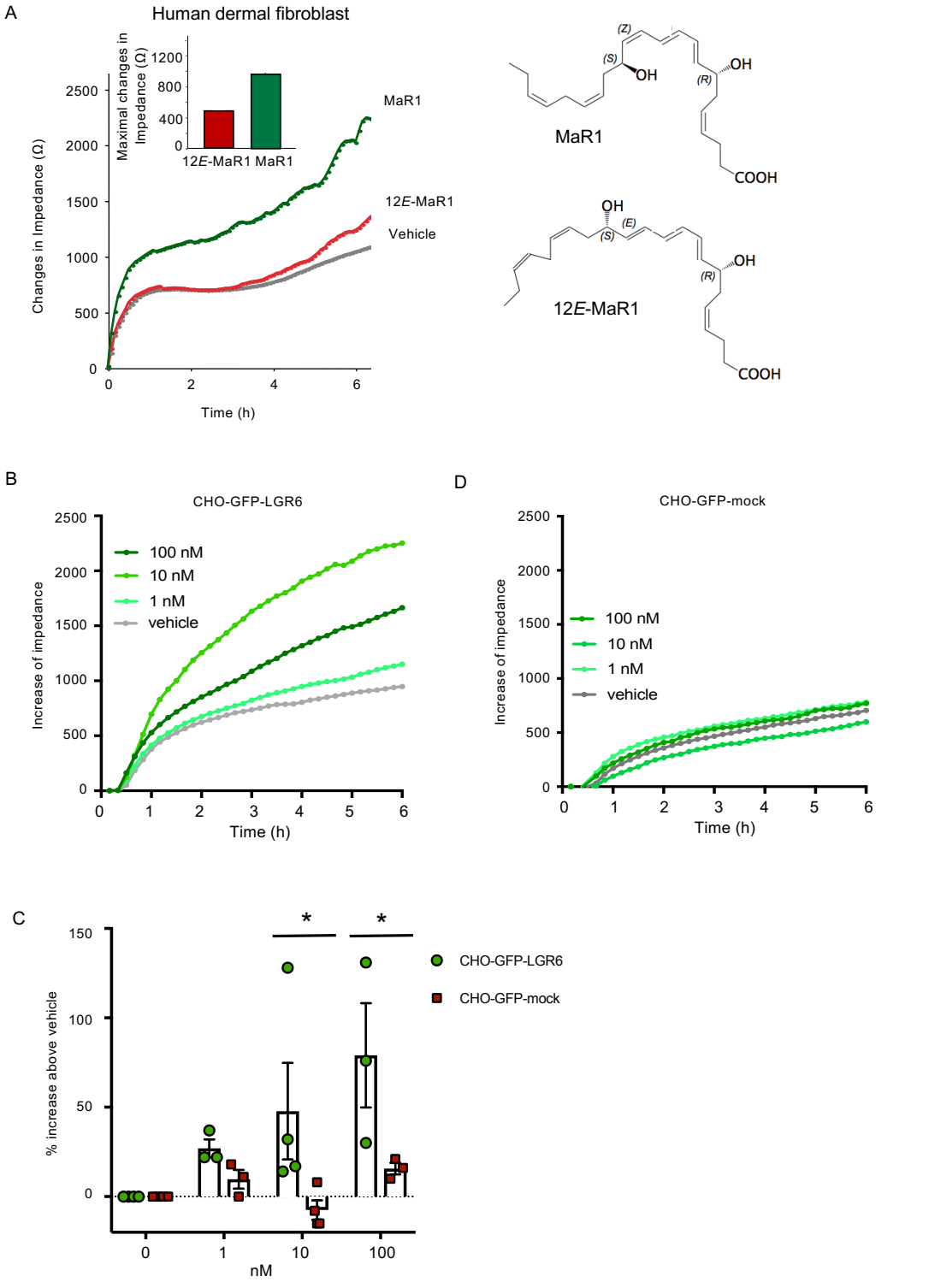

Supplemental Figure 4. MaR1 stimulates fibroblasts wound repair stereoselectively and epithelial cells in a LGR6-dependent manner

(A) Human dermal fibroblasts, (B-D) GFP-LGR6 or GFP-mock vector transfected CHO cells were wounded (1,250 mA, 64KHz, 30 seconds). Changes of impedance (Ω) was recorded every 10 min using ECIS (6h at 37 ºC) on 8W1E electrode arrays following addition of (A) 10 nM MaR1, 12*E*-MaR1 or vehicle control; (B-D) 1-100 nM MaR1 or vehicle control. Results are (A, B, D) representative real-time tracings from n=3-4; (A, *inset*) mean of n=3; (C) mean±SEM; n=3-4. *P<0.05, CHO-GFP-LGR6 vs CHO-GFP-mock; two-way ANOVA with Tukey's multiple comparisons test.

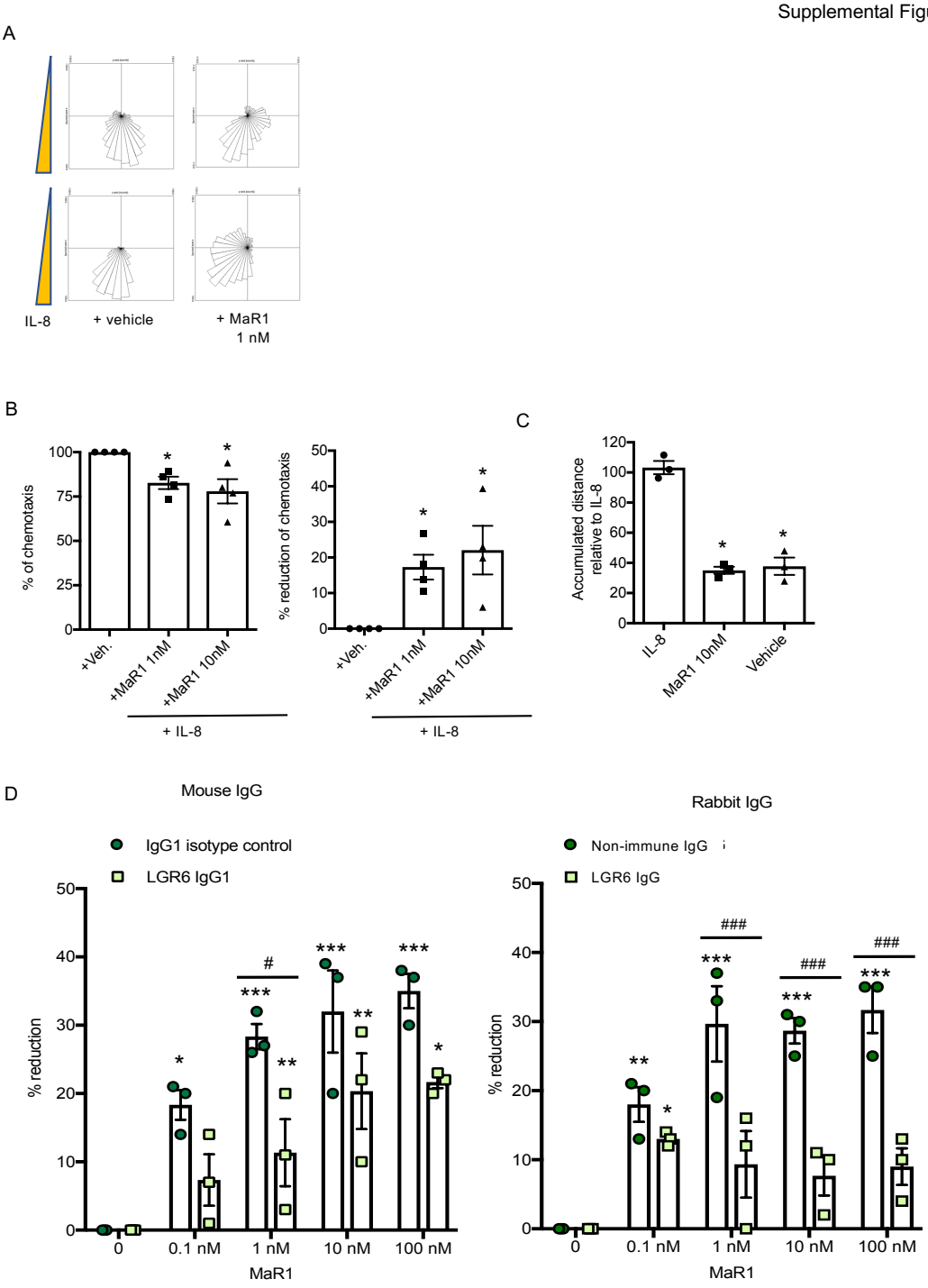

Supplemental Figure 5. LGR6-mediated MaR1 actions on human PMN

(A-C) PMN chemotaxis. Freshly isolated human PMN were incubated with 1 or 10 nM MaR1 or vehicles (PBS + 0.1% ethanol) for 10 minutes. Chemotaxis toward a IL-8 (10nM) gradient (10nM) in Ibidi Chemotaxis μ-Slide was monitored in real time for 2h. (A) Representative rose plots from 2 representative donors. (B) % chemotaxis and % reduction of IL-8-initiated neutrophil chemotaxis; mean±SEM, n=4. *p<0.05, vs. IL-8 + vehicle. (C) Accumulated distance relative to IL-8 (100%); mean±SEM, n=3. *p<0.05, vs. IL-8. One-way ANOVA.

(D) PMN transmigration. IL-8 (10 nM, 30 μl) were placed in the bottom chamber of the Neuro Probe chemotaxis chambers. CFSE-lableled PMN ($5x10^6$/ml) was incubated with mouse anti-human LGR IgG1, rabbit anti-human LGR6 IgG or isotype controls (1:100 dilutions) for 30 min at RT, followed by addition of MaR1 (0.1-100 nM) or vehicle for 15 min. PMN (25 μl) were then added to the top the filters to initiate chemotaxis toward IL-8 for 2h (37°C in 5% CO_2). Migrated cells in the bottom chambers were quantified using fluorescence. Results are mean±SEM, n=3. *p<0.05, **p<0.01, ***p<0.001, vs vehicle controls; $^{\#}p$<0.05, $^{\#\#\#}p$<0.001, vs. isotype controls (mouse) or non-immune IgG (rabbit); two-way ANOVA with Tukey's multiple comparisons test.

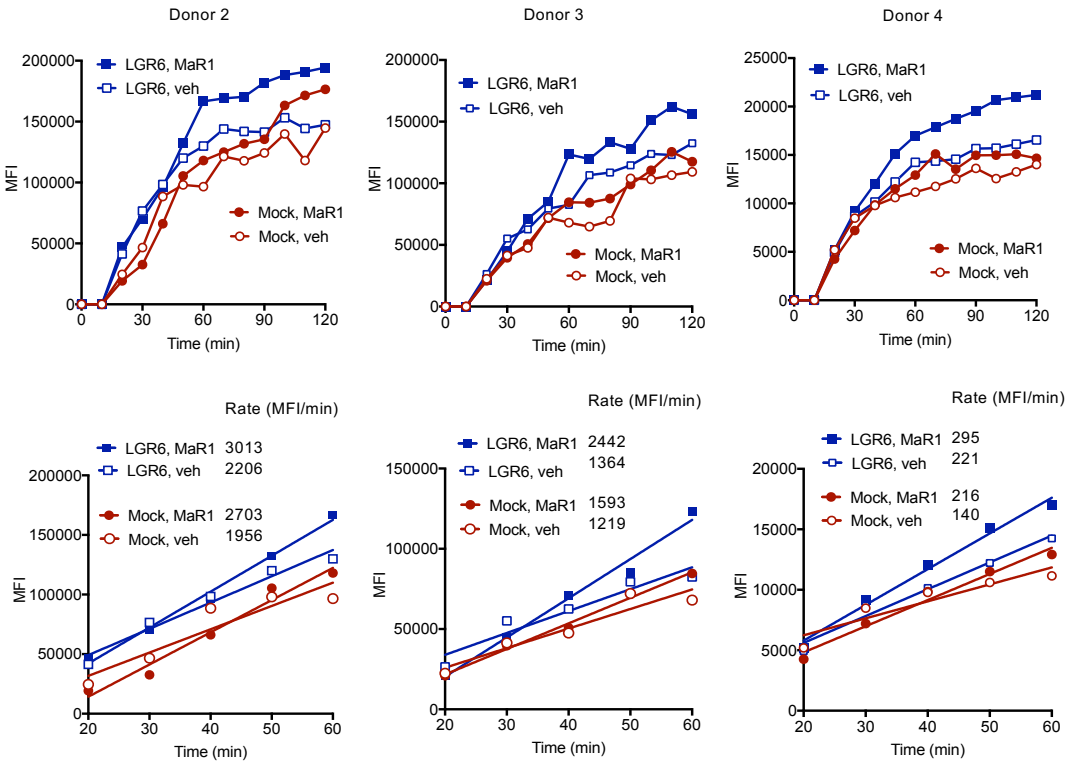

Supplemental Figure 6. Overexpression of human LGR6 enhances MaR1 actions in stimulating macrophage phagocytosis

Human MΦ were transfected with human LGR6 or mock plasmid. Phagocytosis was carried out as in Figure 4A. Results are mean fluorescence intensity (MFI) (top panels) and kinetics of phagocytosis (bottom panels) from 3 separate donors.

A

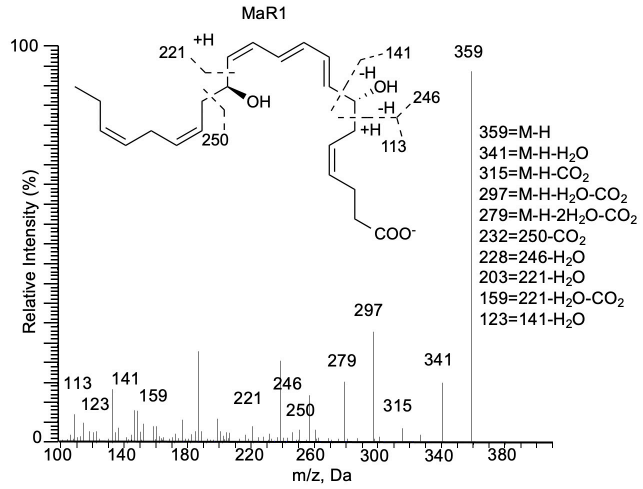

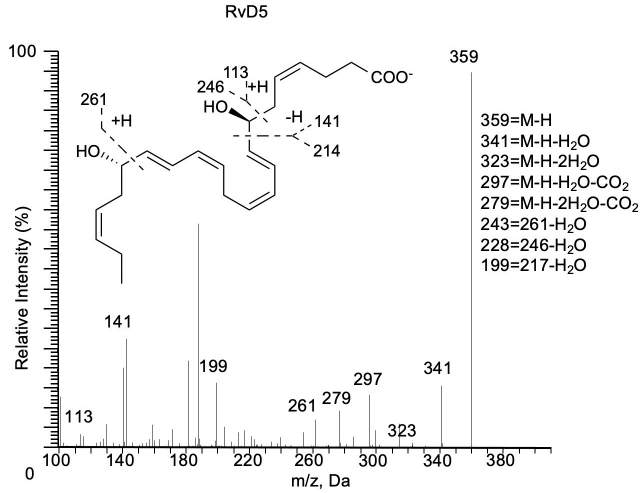

B

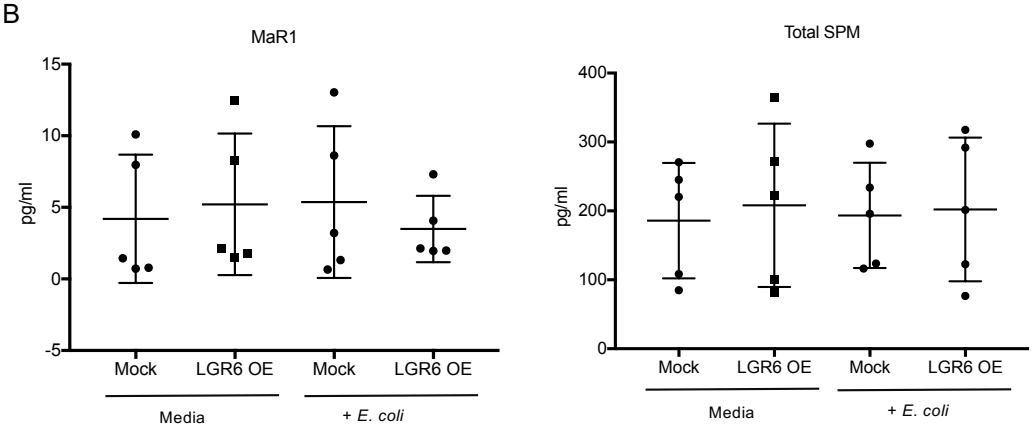

Supplemental Figure 7. LM/SPM metabololipidomics of human macrophages: LGR6 overexpression with *E. coli* incubation.

Human MΦ were transfected with human LGR6 plasmid or a mock plasmid. MΦ ($1x10^6$ cells) were then incubated with *E. coli* ($5x10^7$ CFU) for 1h. Incubations were terminated using ice-cold methanol, extracted and LM/SPM levels determined using mass-spectrometry-based metabololipidomics (see Methods).

(A) Representative MS-MS of MaR1 and RvD5.

(B) MaR1 and total SPM levels (pg/ml; $0.5x10^6$ cells); mean±SEM, n=5. No statistical significances were obtained among groups; one-way ANOVA with Tukey's multiple comparisons test.

Please see Supplemental Table 3 for a tabular presentation of the results in panel (B).

A

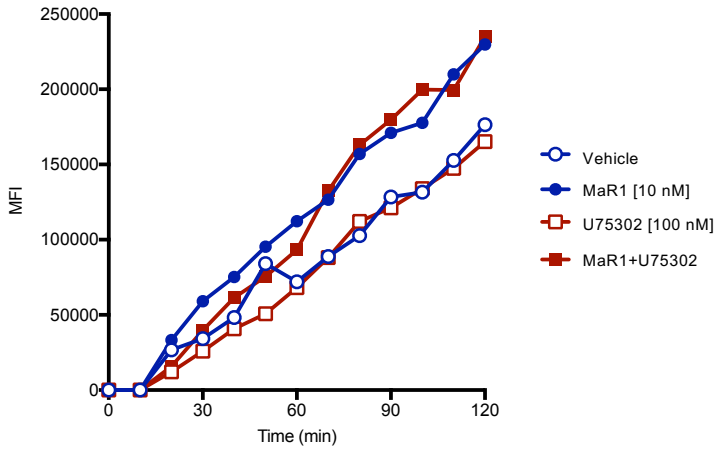

B

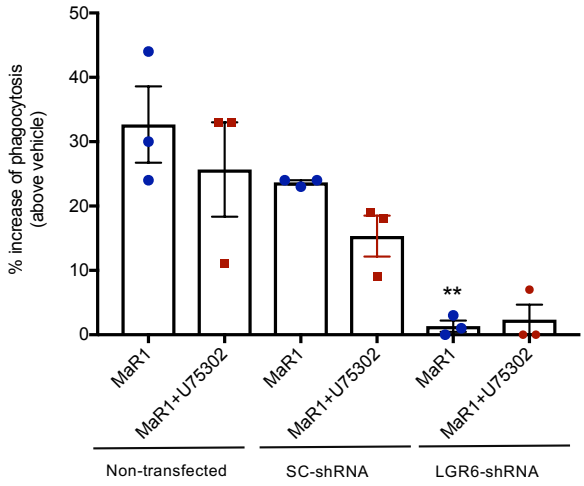

Supplemental Figure 8. MaR1-stimulated phagocytosis with human macrophages is not altered by an BLT1 antagonist.

Human MΦ (non-transfected, non-target siRNA or LGR6 siRNA-transfected) were plated onto chamber slides (0.1 x10^6 cells/well), incubated with a BLT1 antagonist (U75302; 100 nM) or vehicle for 10 min, followed by MaR1 (10 nM) or vehicle control for 15 min at 37°C. BacLight Green-labeled *E. coli* was then added to initiate phagocytosis. Fluorescent images were then recorded every 10 min for 60 min. Three separate experiments were carried out. In each experiment, 4 fields (40X) per condition (per well) were recorded.

(A) Results are mean fluorescence intensity (MFI)/cell of 4 fields/condition from one representative experiment with non-transfected MΦ.

(B) Results are % increase of phagocytosis above vehicle controls; mean±SEM, n=3. **P<0.01, vs MaR1 in non-transfected, SC-shRNA groups. No statistical significances were obtained between MaR1 and MaR1+U75302 in non-transfected, SC-shRNA and LGR6-shRNA groups; two-way ANOVA with Bonferroni's multiple comparisons test.

A

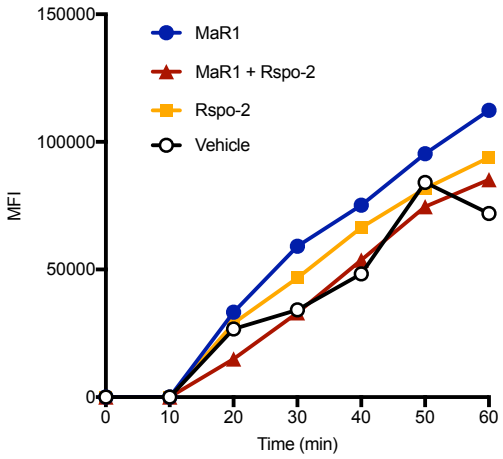

B

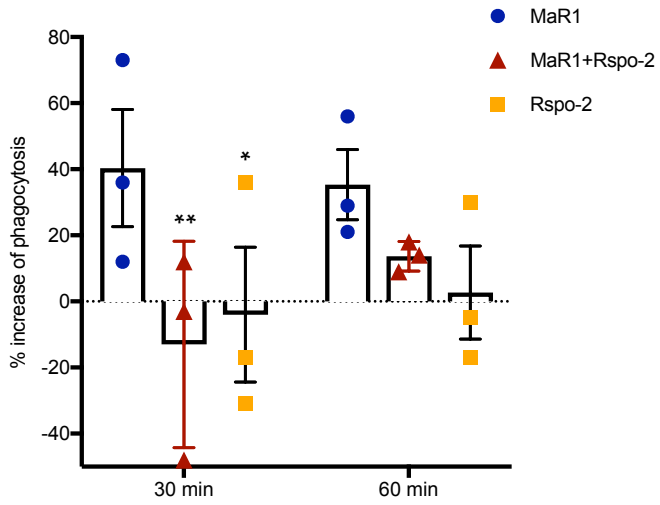

Supplemental Figure 9. R-spondin-2 reduces MaR1-stimulated phagocytosis with human macrophages.

Human MΦ were plated onto chamber slides (0.1 x10^6 cells/well), incubated with R-spondin-2 (Rspo-2; 10 nM) or vehicle for 10 min, followed by MaR1 (10 nM) or vehicle control for 15 min at 37°C. BacLight Green-labeled *E. coli* was then added to initiate phagocytosis. Fluorescent images were then recorded every 10 min for 60 min. Three separate experiments were carried out. In each experiment, 4 fields (40X) per condition (per well) were recorded.

(A) Results are mean fluorescence intensity (MFI)/cell of 4 fields/condition from one representative experiment.

(B) Results are % increase of phagocytosis above vehicle controls; mean±SEM, n=3. *P<0.05, **P<0.01, vs MaR1 at 30 min; two-way ANOVA with Bonferroni's multiple comparisons test.

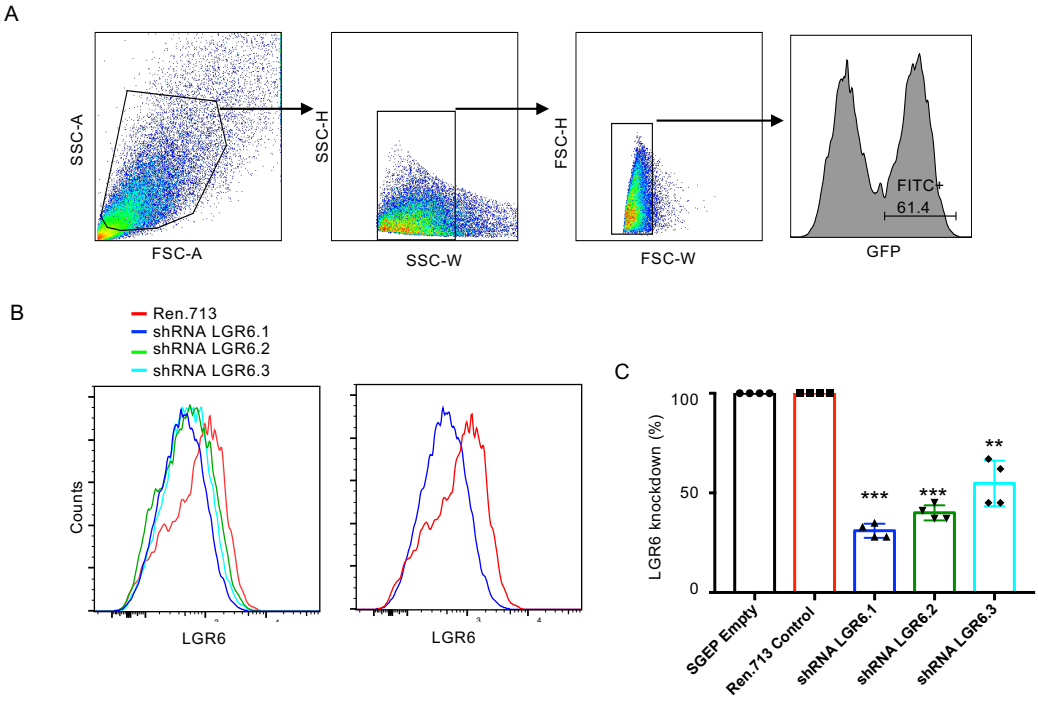

Supplemental Figure 10. Stable LGR6 knockdown in HEK cells and MaR1 signaling with peripheral blood leukocytes

Stable LGR6 knockdown in HEK293 cells.

(A) Gating strategy for flow cytometry: HEK 293 cells were gated on FSC and SSC dot plots (left panel), then GFP positive (GPF+) populations were selected on the histograms (right panel).

(B) LGR6 expression was determined within the GFP+ population. Results are representative histograms of Renilla 713 shRNA control and different clones of LGR6 reporter knockdown. The left and right panels were plotted using the same dataset. The right panel shows Ren.713 with one of the shRNA LGR6 clones (#1) that's selected for further investigation.

(C) Each shRNA LGR6 reporter knockdown clone was calculated and compared to controls Renilla 713 shRNA control and empty mock SGEP vector. Results are mean±SEM; n=4. ***p*<0.01, ***P<0.001 vs. controls shRNA Renilla 713 or mock vector; one-way ANOVA with Tukey's multiple comparisons test.

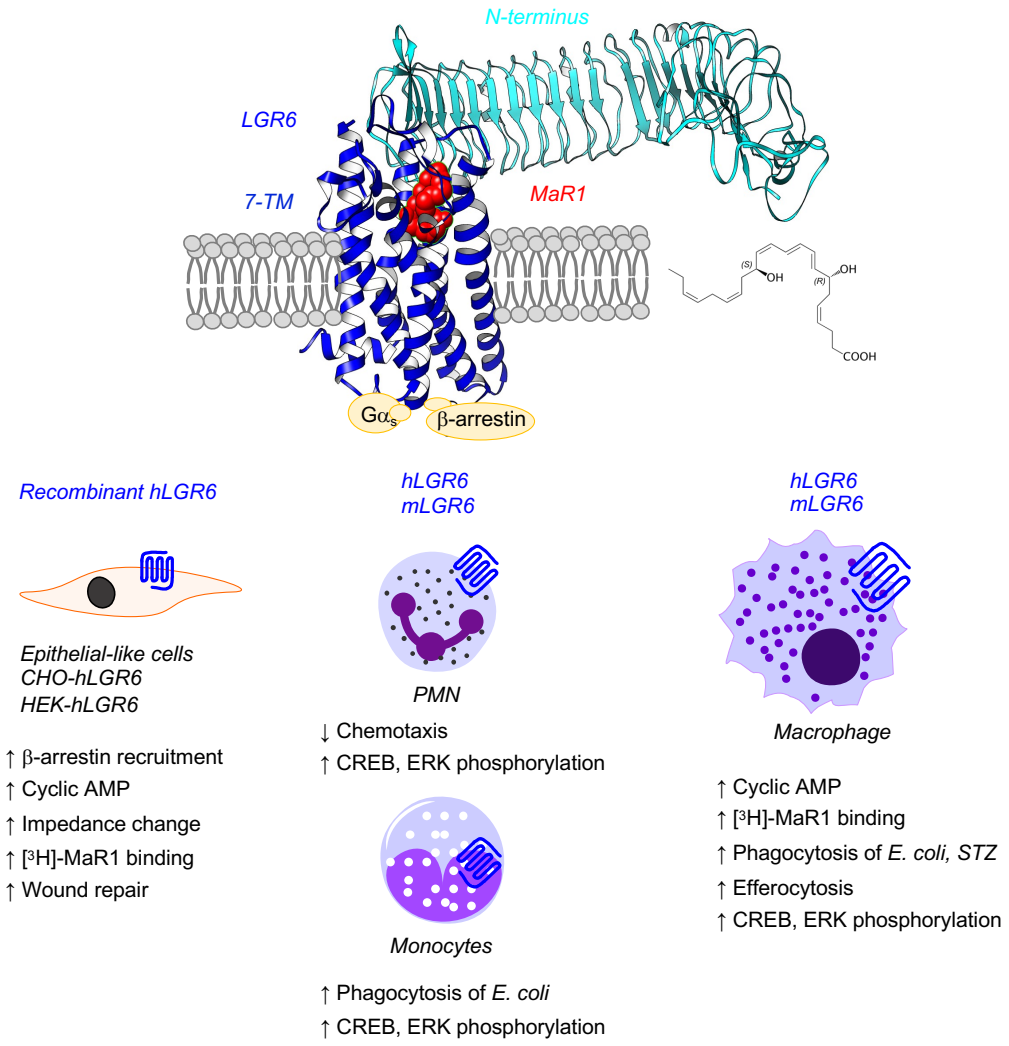

Supplemental Figure 11. Illustration of MaR1-LGR6 dependent signaling and functions. Predicted LGR6 structure and MaR1 docking using UCSF Chimera (https://www.cgl.ucsf.edu/chimera/). LGR6 consists of N-terminus with leucine-rich repeats (light blue), and seven transmembrane domains (7-TM; dark blue). MaR1 3D structure is depicted in red, and predicted to interact with the transmembrane domains of LGR6.

MaR1-LGR6 interactions initiate G protein coupling and response signals including impedance change, cAMP increase with recombinant LGR6. With phagocytes, MaR1-LGR6 interactions stimulate key pro-resolving functions with human and mouse MΦ, i.e., enhancing MΦ phagocytosis and efferocytosis. In addition, MaR1-LGR6 evoked phosphorylation signals with human and mouse monocytes and PMN, as well as limiting human PMN chemotaxis.

Graphic Abstract

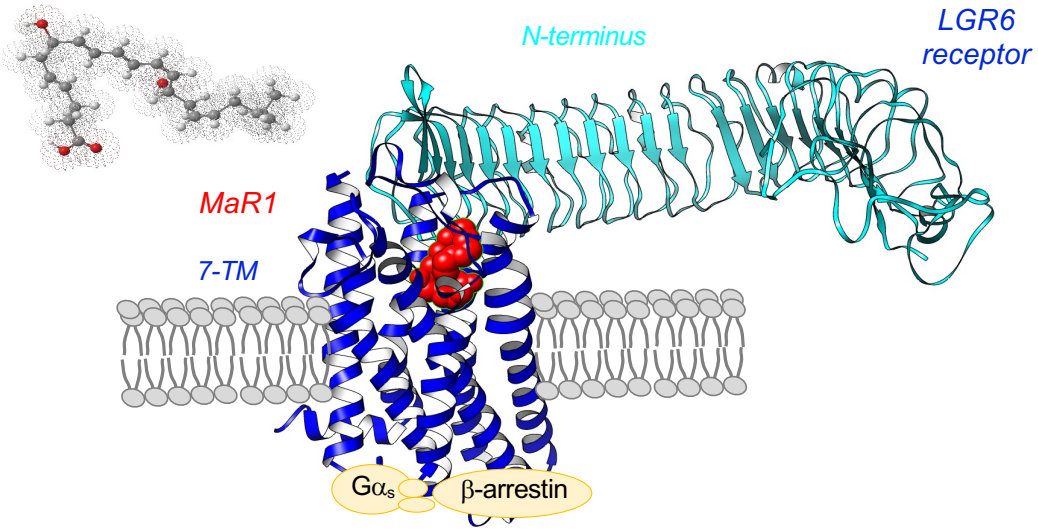

PMN

Chemotaxis

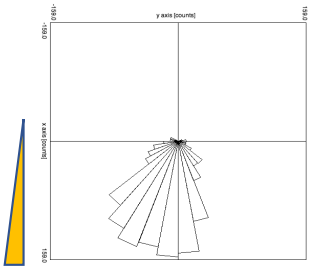

PMN
Monocytes
Macrophages

Phosphorylation

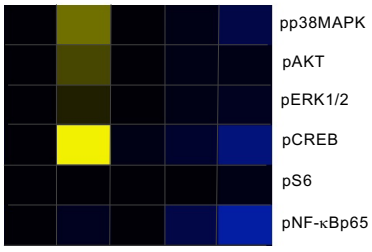

Monocytes
Macrophages

Phagocytosis